Bio-nanohybrids of quantum dots and photoproteins facilitating strong nonradiative energy transfer

Safak Seker, Urartu Ozgur; Mutlugun, Evren; Hernandez-Martinez, Pedro Ludwig; Sharma, Vijay K.; Lesnyak, Vladimir; Gaponik, Nikolai; Eychmüller, Alexander; Demir, Hilmi Volkan

2013

Safak Seker, U. O., Mutlugun, E., Hernandez-Martinez, P. L., Sharma, V. K., Lesnyak, V., Gaponik, N., et al. (2013). Bio-nanohybrids of quantum dots and photoproteins facilitating strong nonradiative energy transfer. Nanoscale, 5(15), 7034-7040.

https://hdl.handle.net/10356/81855

https://doi.org/10.1039/c3nr01417g

Journal Name

Dynamic Article Links ►

Cite this: DOI: 10.1039/c0xx00000x

www.rsc.org/xxxxxx

ARTICLE TYPE

Bio-Nanohybrids of Quantum Dots and Photoproteins Facilitating Strong Nonradiative Energy Transfer

Urartu Ozgur Safak Seker,[a,b,c,‡,*] Evren Mutlugun,[a,b,c,‡] Pedro Ludwig Hernandez- Martinez,[a,b] Vijay K. Sharma,[b] Vladimir Lesnyak,[d,e] Nikolai Gaponik,[d] Alexander Eychmüller,[d] and Hilmi Volkan Demir[a,b,*]

Received (in XXX, XXX) Xth XXXXXXXXX 20XX, Accepted Xth XXXXXXXXX 20XX
DOI: 10.1039/b000000x

‡ These authors have contributed equally

*Corresponding authors

Present Address: [c]Massachusetts Institute of Technology, Synthetic Biology Center, 500 Technology Square, NE47-257, Cambridge MA, [e] Instituto Italiano di Tecnologia, Via Morego 30, 16163 Genova, Italy

Utilization of is crucial for the life cycle of many organisms. Also, many organisms can create light by utilizing chemical energy emerged from biochemical reactions. Being the most important structural units of the organisms, proteins take a vital role in the formation of the light in the form of bioluminescence. Such photoproteins have been isolated and identified for a long time; the exact mechanism of their bioluminescence is well established. Here we show a biomimetic approach to build a photoprotein based excitonic nanoassembly model system using colloidal quantum dots (QDs) for a new bioluminescent couple to be utilized in biotechnological and photonic applications. We are concentrated on the formation mechanism of the nanohybrids using a kinetic and thermodynamic approach. Finally we propose a biosensing scheme with an ON/OFF switch using the QD-GFP hybrid. QD-GFP hybrid system promises strong exciton-exciton coupling between the protein and the quantum dot at a high efficiency level, possessing enhanced capabilities of light harvesting, which may bring new technological opportunities to mimic biophotonic events.

Introduction

Bioluminescence is a biological activity of different organisms ranging from bacteria to plants[1-4]. Unlike the photoluminescence and fluorescence, bioluminescence is a cold body radiation triggered by a chemical reaction in the biological organism. In bioluminescence, a molecule is produced at the excited state, which finally emits a photon during relaxation. Among those molecules utilized during bioluminescence, green fluorescent protein is well known, well characterized photoprotein, which has been widely used in biolabeling. [5, 6]

GFP and GFP mutants based on Förster-type resonance energy transfer (FRET) were utilized to track a targeted biological event within a living cell, where the FRET processes between the GFP and its mutants are utilized as reporters. [7-9] Naturally occurring systems exhibit their own strength by means of physical, mechanical and optical properties. They were formed after a long evolutionary process, which gave them strength and flexibility. Therefore, photoproteins are unique owing to simplicity of their synthesis and optical adjustability through genetic engineering tools. On the other side, technologically improved approaches can solve an actual problem that nature does not necessarily need to deal with. At this stage, nanocrystals were synthesized and being offered for utilization in technological applications.[10-12] A hybrid of these two components will offer new possibilities; by using the unique optical properties of QD and introducing the flexibility, genetic tenability and biocompatibility of GFP, a promising hybrid system for biomedical and biochemical applications can be favored. A hybrid of these two components offers new possibilities; by using the unique optical properties of QD and introducing the flexibility, genetic tenability and biocompatibility of GFP, a promising hybrid system for biomedical imaging applications and biochemical applications can be favored. Initial studies have successfully presented bionanohybrid approach for the assembly of protein/photoprotein-QD conjugates.[10, 13-16] However, investigation of the nanohybrid formation mechanism by means of the kinetics and thermodynamics of the interaction of the QD with proteins will increase the control over the assembly. Such an investigation may contribute to the understanding of molecular interactions for future engineering of the nanohybrid using tool of biochemistry and material science.

In this study we are proposing a route for QD-GFP nanohybrid assembly. A distinct approach from the previous studies is that, instead of the fluorescence intensity measurements that needs to be normalized regarding the emitting species, [17] and though can

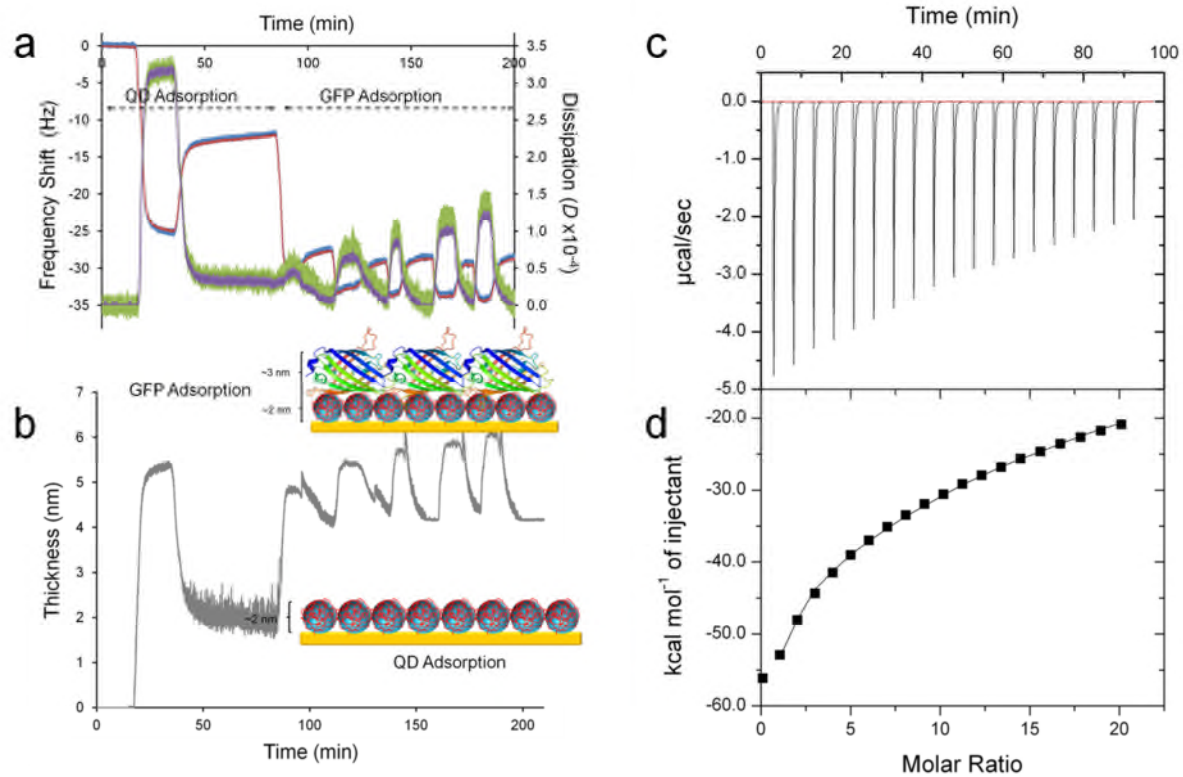

Fig.1 QCM-D analysis of the binding of QDs and GFP-6X-His in a sequential manner. a) Frequency shift upon adsorption quantum dots and GFP-6X-His (blue line) with a viscoelastic model fit (red line) and dissipation change upon adsorption of the nonentities and GFP on cysteamine modified gold electrode (green line) along with the viscoelastic model fit (purple line). b) Thickness monitoring of the layer-by-layer assembly of the QDs and GFP-6X-His. c) ITC Titration curves of GFP-6X-His onto QD after each injection. d) Calculated area under the ITC titration curves and model fitting of a single interaction model using the software provided along with the instrument.

be deceptive without a calibration, a more accurate method; time resolved fluorescence spectroscopy was used to follow emission kinetics of the FRET facilitating species. FRET process was characterized to determine donor and acceptor lifetimes, regardless of the amounts of the FRET facilitating species. Kinetics and thermodynamics of the formation of the nano-bio hybrid structure was investigated to understand how to control the supramolecular interaction within a nanohybrid. Kinetic investigations also led to determine the distance between each components of the nanohybrid, which was verified theoretically as well. Not only the kinetic analysis but also X-ray photoemission spectroscopy and thermogravimetric analysis were carried out to probe the formation of the GFP-QD nanocomposites. Functional analysis of the GFP-QD revealed a high FRET efficiency of 70%, and we have showed up to 15-fold enhancement on the emission of the GFP when conjugated with QDs due to the strong excitonic interaction possessing the nonradiative energy transfer. Exploiting the strong nonradiative energy transfer within nanohybrid, a protease sensor working upon a temperature depended ON/OFF switch was demonstrated as a tool for temperature based protease sensor applications. In this work, a bottom up approach for the nanohybrid design, which mimics the aequorin-GFP pair existing in the jellyfish *Aequorea victoria*, with high controllability and adjustability promising a wide range of applicability, is demonstrated.

Experimental Section

Preparation of Nanocrystals

ZnCdSe quantum dots have been synthesized according to the previously reported work. [18]

Expression and Purification of GFP-6X-Histag

gfp gene was first amplified using P1 and P2 primers (see supporting information) carrying NcoI and BamHI restriction sites at their 5' respectively. P2 primer also contained sequences encoding for trypsin protease clevage site (STRTDEG) and Histag (HHHHHH) at its 3'. Amplified gene was cloned into a pet11D vector digested with NcoI/BamHI. *Escherichia coli* BL21 strain was transformed with pet11D encoding engineered *gfp*. Purified engineered GFP was attached to the QD surface through coordination with histag.

Quartzy Crystal Microbalance -Dissipation Analysis

The interaction of the GFP-6X-His with the QDs was tested using Quartz crystal microbalance Q-Sense E1 (from Q-Sense Company, Frolunda, Sweden). First the surface of the gold QCM-D crystals was activated using cysteamine and then using carbodiimide chemistry, QDs were attached to the functionalized

sensor surface. After ensuring the attachment of the QDs with the observation of frequency change, the GFP-6X-His was flown on the surface and the change in the frequency shift at varying GFP concentrations was recorded.

Isothermal Titration Calorimetry

Experiments were carried out using a Microcal 200 equipment (GE Healthcare, Austria). Quantum dots at 15 μM concentrations were kept in the titration vessel while the 150 μM GFP-6X-Histag was injected into the QD colloid. The Thermal titration was performed at 25 °C and in 0.5X PBS buffer at 500 rpm. ITC data were fitted to a single interaction function using Origin 7 supplied along with the ITC200. Following the runs, the instrument was automatically and manually cleaned with methanol, detergent and DI water.

Time-resolved Photoluminescence

Experiments were performed using PicoQuant Fluo Time 200 time-correlated single photon counting system. A laser diode operating at 375 nm has a repetition rate of 80 MHz with 200 ps width. The lifetimes have been extracted by the data acquisition software PicoHarp 300 with a <10 ps lifetime resolution.

Steady-state Photoluminescence and Absorption:

Cary Eclipse fluorescence spectrometer and Cary UV-Vis spectrometer were used in the experiments.

Results and Discussions

Kinetic and Thermodynamic Analysis of GFP-QD Nanohybrid Formation

In order to investigate the interaction modes between the QD and GFP, we carried out a quartz crystal microbalance (QCM-D) based affinity analysis where we monitored the binding kinetics of the GFP molecules onto the surface decorated with QDs as presented. [19] In this setup, ZnCdSe QDs were first immobilized on the gold surface of the QCM-D sensor by means of carbodiimide mediated covalent bonding. The unfilled parts of the sensor were blocked with 1 mM ethanolamine to prevent the nonspecific attachment of the QDs on modified sensor surface. Following the coverage of the QCM-D sensor surface, the GFP-6X-His molecule was sent into the flow cell of the QCM-D where the QD functionalized sensors were placed. The adsorption and desorption of the molecules were monitored for five varying concentrations of GFP-6X-His, ranging from 2 to 10 μM. The interaction analysis was carried out using a simple interaction model, which yielded an affinity constant of 0.9 μM, indicating a strong interaction between the GFP-6X-His and QD. QCM-D does not only provide the binding isotherms but also gives the dissipation data of the adsorbed GFP layer onto QDs. The dissipation data indicates here that the interaction between the QD and GFP-6X-His yielded in the formation of a GFP film on top of the QD without denaturation of the GFP.

Using the dissipation data (Figure 1a) for fitting into a Voigt viscoelastic model[20], the thickness of the GFP film was calculated to be as high as ~3 nm (see Figure 1b). Considering the GFP has a barrel structure composed of sheets and helices with a total diameter of 30 to 40 Å [21], the results suggest that the GFP-6X-His molecules interact with the QD by the longer side of the barrel, as represented in Figure 2. Also, the dissipation change throughout the interaction experiment suggests that the QD-GFP film entraps water molecules, preventing the GFP from denaturing upon interaction with the semiconductor surface, which otherwise would lead to improper FRET distance between the QD-GFP.

Since the final design of the QD-GFP nanohybrids is water dispersible colloidal entities, besides confirming the thickness of GFP and its affinity on a solid surface, a solution based biophysical approach, isothermal titration calorimetry (ITC) was employed to probe the strength of the interaction between QD-GFP. In the experimental setup GFP-6X-His was injected into ZnCdSe QD solution placed in a reaction chamber made up of a biologically inert alloy. After each injection of the GFP into the reaction chamber of ITC, released energy upon GFP's interaction with QDs was recorded as given in Figure 1c. Peak areas were calculated and fitted to an interaction model supplied by Origin software, which is shown in Figure 1d. From the single mode interaction model, the enthalpy of binding for the QD and GFP-6X-His was calculated as -82 kcal/mol. Although this is a high amount of energy release, we observed a lower affinity desorption constant of 17 μM compared to the QCM-D analysis. This indicates different modes of binding in both experimental cases. The difference in the binding mechanism may arise due to the higher local concentration of QDs in the film as compared to the solution, and these facts may be facilitated by the interaction of the GFP molecules with the QDs. Additionally, through the interaction of the adjacent protein molecules, adsorbed amount of proteins on the QD surface can be increased.

Although we have strong evidence of the interactions between GFP-6X-His and ZnCdSe QDs, we further investigated the chemical interactions of the GFP with the QDs at the atomic level using the X-ray photoemission spectroscopy (XPS). As presented in XPS data in the supporting information part, the high resolution C 1s & O 1s spectra for the GFP, ZnCdSe QDs, and the composite were acquired. Due to the changes in the XPS spectrum of GFP-QD mixture and the existence of additional peak compared to the GFP and QD alone, we suspect that the imidazole ring of the histidine tag at the end of GFP gets in contact with the QD through supramolecular interactions.

Cite this: DOI: 10.1039/c0xx00000x

www.rsc.org/xxxxxx

ARTICLE TYPE

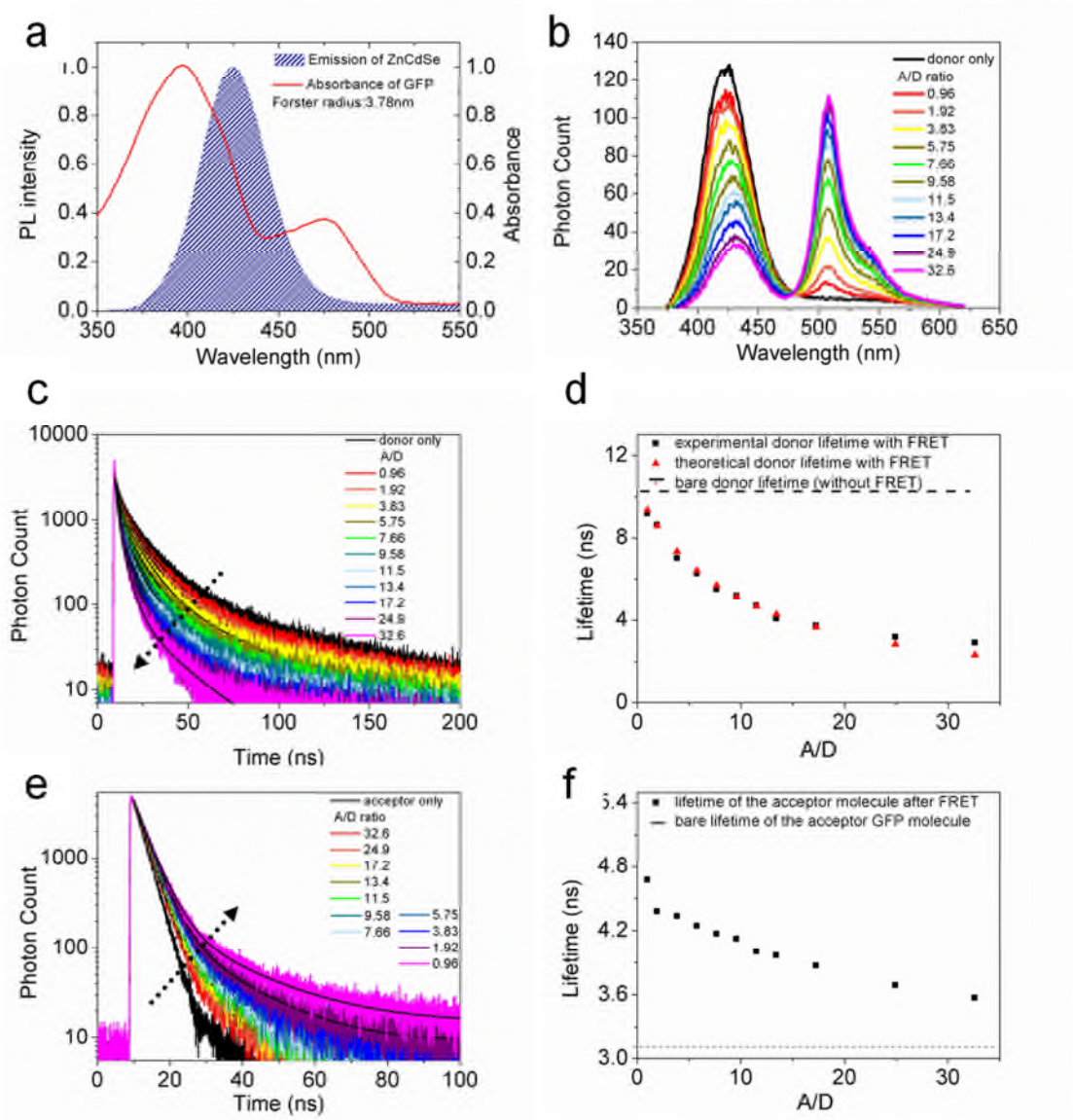

Fig.2 a) Spectral overlap of ZnCdSe QD and GFP, red line shows the absorption spectrum of the GFP and the blue shadowed area represents the emission spectrum of the ZnCdSe QDs. b) Photoluminescence spectra of the donor-acceptor QD-GFP system with changing A/D concentration ratio (excitation at 315 nm) c) Time-resolved photoluminescence decays of the donor, changing with the A/D ratio (at 422 nm). d) Donor lifetimes, extracted from time-resolved photoluminescence decays, and theoretically predicted, as a function of the A/D ratio. e) Time-resolved photoluminescence decays of the acceptor changing with the A/D ratio (at 508 nm). f) Acceptor lifetimes, extracted from time-resolved photoluminescence decays, as a function of the A/D ratio

Experimental and Theoretical Analysis of Nonradiative Energy Transfer in GFP-QD Nanohybrid

Energy transfer mediated light harvesting was first performed at steady state conditions. Later, time-resolved photoluminescence measurements were employed to monitor the energy transfer. The steady state measurements demonstrate the effect of the energy transfer from the QDs (D) to GFP (A). As the A/D ratio is increased, we observe a decrease of the emission intensity of the donor QDs, whereas an increase in the acceptor emission is observed as a result of energy feeding from the donor side. A spectral overlap between the emission of the QD (with an emission maximum at 422 nm) and the optical absorption of GFP (maxima at 395 nm and 475 nm) was verified to satisfy FRET as presented in Figure 2a. Steady state fluorescence measurements

were performed to monitor any changes in the emission of QD and GFP before their interactions as well the emission of the nanohybrid structure with the excitation monochromator set at 315 nm. The photoluminescence measurements of the quantum dot-protein composite are shown in Figure 2b. The enhancement of the pure acceptor emission is extracted from the steady state emission data of the GFP in the presence and absence of the donor QDs.

To demonstrate the excitation of the GFP well beyond its absorption, we chose the excitation wavelength at 315 nm, in order to satisfy the spectral overlap conditions at the expected maximum efficiency (Supplementary Figure S4). The enhancement of the acceptor emission was calculated as a function of the acceptor concentration, and presented as A/D concentration ratio.

$$Enhancement = \left[\frac{\int_{480}^{620} I_A^D(\lambda)\, d\lambda}{\int_{480}^{620} I_A(\lambda)\, d\lambda} - 1 \right] \quad (1)$$

Here, I_A is the intensity of the acceptor GFP in the absence of the donor QD and I_A^D is the intensity of the acceptor in the presence of the donor. The wavelength interval from 480 to 620 nm was chosen since the emission spectrum of GFP lies within this region. Carrying out the analysis, we observed an enhancement of the acceptor photoluminescence of up to 15 folds corresponding to an A/D ratio of ~5, which is consistent with the geometrical factors given the size of the GFP and the QDs. As the amount of GFP is further increased, the overall enhancement decreases because the system is converging to the case of acceptor only.

Using time-resolved photoluminescence spectroscopy fluorescence emission lifetimes of the donor, the acceptor and the hybrid was monitored at the donor and the acceptor emission wavelengths, 422 and 508 nm, respectively given in Figure 2c-2f. A dramatic change in the QD fluorescence lifetime was noted while changing the GFP concentration and keeping the QD concentration the same, which points at an efficient nonradiative energy transfer from QD to GFP. Starting with the A/D concentration ratio of 0.96, we observed the photoluminescence decays getting faster with increasing A/D ratio up to 32.6, where we observed adsorption saturation.

The lifetime modification kinetics of both donor and acceptor with respect to any change of any given FRET pair was found to follow a biexponential behaviour. The lifetime of the donor changes from 10.33 to 2.91 ns as we increase the A/D concentration ratio. Similarly, we carried out the lifetime measurements for the acceptor molecules, where a dramatic increase in the acceptor lifetime was observed because of the energy feeding from the donor to the acceptor. Throughout the A/D ratios we explored, an increase in the acceptor lifetime was observed. We measured lifetime modifications ranging from 3.57 to 4.67 ns for the GFP (The bare lifetime of the GFP, 3.11 ns, is shown with dotted line in Figure 2f). The trend of the modification of the lifetime is as expected due to the fact that as we increase the acceptor to donor concentration, we decrease the energy transferred per acceptor, thus the system is evolving to acceptor only case, which is in agreement with the experimental observation.

The observed FRET efficiency due to the dipole interaction of the donor-acceptor pairs was calculated using Equation. 2

$$\eta = 1 - \frac{\tau_{DA}}{\tau_D} \quad (2)$$

Where τ_{DA} is the lifetime of the donor in the presence of the acceptor and τ_D is the bare lifetime of the donor. As a result of the energy transfer, we observed FRET efficiencies of up to 70% for our QD-GFP complex. In connection with the theoretical model based on the dipole-dipole interaction, the efficiency levels are in good agreement with the experimentally observed values. In the theoretical approach, we considered energy transfer from ZnCdSe QDs to multiple GFP molecules under exciton-exciton interaction. Within the simplest rate model, the number of excitons (N_{exc}) generated in the QD, under constant illumination (steady-state condition), is given by [22]:

$$-\left(\gamma_{exc}^D + \gamma_{trans}^{tot}\right) N_{exc}^D + I_D = 0 \quad (3)$$

where N_{exc}^D is the number of excitons in the donor, I_D is the exciton generation rate due to the light excitation, and $\gamma_{exc}^D = \gamma_{exc,rad}^D + \gamma_{exc,non-rad}^D$ is the donor exciton recombination rate in the absence of acceptor. $\gamma_{exc,rad}^D$ and $\gamma_{exc,non-rad}^D$ are the radiative and nonradiative components of respectively. $\gamma_{trans}^{tot} = n\gamma_{trans}$ is the total energy transfer rate between the donor and multiple acceptors. γ_{trans} is the number of acceptors and is the energy transfer between one donor and one acceptor. By substituting into Eqn. 3, it can be written as:

$$-\left(\gamma_{exc}^D + n\gamma_{trans}\right) N_{exc}^D + I_D = 0 \quad (4)$$

One then defines:

$$\gamma_{DA}^D = \left(\gamma_{exc}^D + n\gamma_{trans}\right) \quad (5)$$

where γ_{DA}^D is the donor exciton lifetime in the presence of energy transfer. For the energy transfer rate between ZnCdSe QD and GFP,

$$\gamma_{trans} = \gamma_{exc}^D \left(\frac{R_0}{r}\right)^6 \quad (6)$$

where R_0 is the Förster radius for the D-A pair and r is the separation distance between ZnCdSe QD and GFP. Therefore Eqn. 5 is given by

$$\gamma_{DA}^D = \gamma_{exc}^D \left(1 + n\left(\frac{R_0}{r}\right)^6\right) \quad (7)$$

In terms of lifetimes,

$$\tau_{DA}^{D} = \frac{\tau_{exc}^{D}}{1 + n\left(\frac{R_0}{r}\right)^6} \quad (8)$$

Here using experimental data, we extracted the effective distance between the QD-GFP to be 5.49 nm in average, which is reasonable when compared with the QD diameter of 4 nm and GFP diameter of ~ 3nm.

The enhancement in the FRET efficiencies does not directly reflect the observed light harvesting enhancement. This is because, as more and more acceptors are introduced, there are more nonradiative channels created for the donor to transfer energy, which results in high FRET efficiencies. On the other side, the light harvesting is optimal up to a certain number of acceptors per a given donor (~5:1, for our system). When A/D is further increased, the amount of light harvesting is decreased, since the system is evolving towards an acceptor only system.

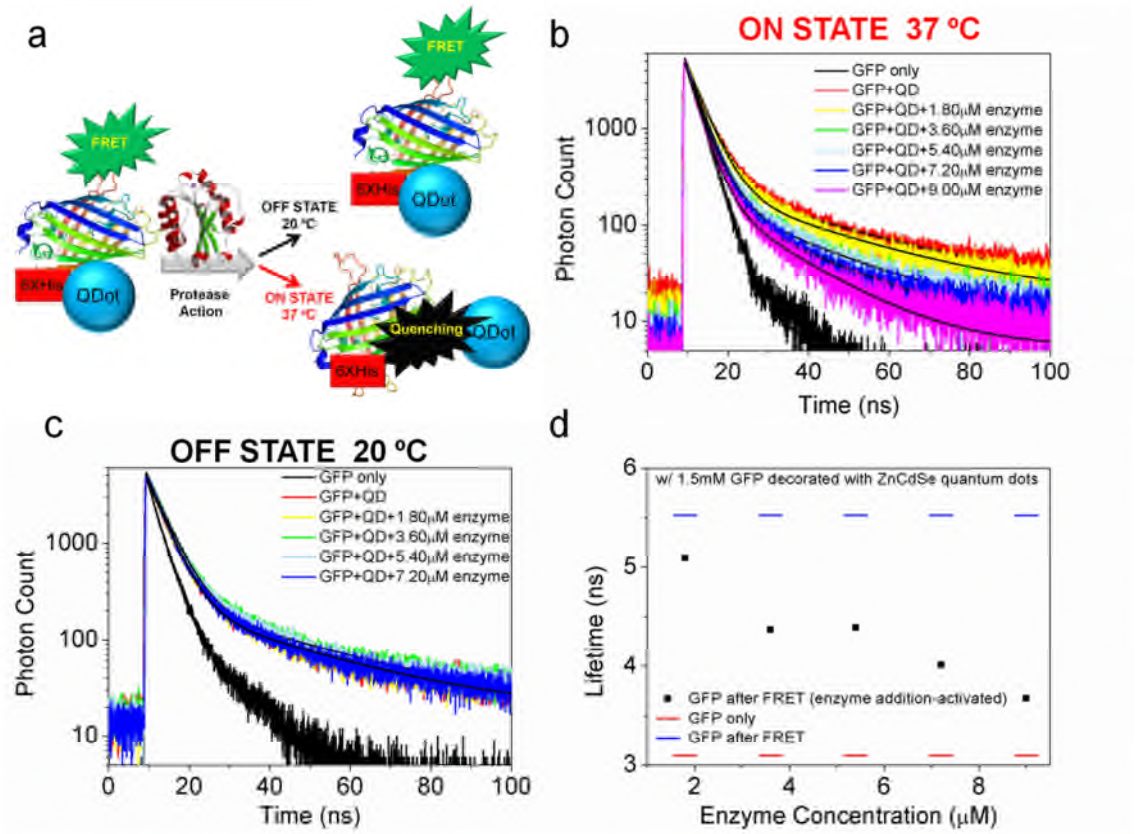

Fig.3 a) Schematic representation of the ON/OFF state sensing of the nanohybrid structure in response to the protease action triggered by temperature b) Photoluminescence decays of the GFP only, GFP with FRET, and GFP in ON state of the enzyme c) Photoluminescence decays of the GFP only, GFP with FRET, and GFP in OFF state. d) Lifetime modifications of the GFP only, GFP with FRET, and GFP after enzyme action.

QD-GFP Based Protease Sensor with a Thermal ON/OFF Switch

The well established FRET process in GFP-QD nanocomposite is utilized as a protease sensor with a ON/OFF state temperature switch as given in schematic in **Figure 3a**. As FRET process strongly depends on the distance between the donor and acceptor species, any modification in the distance between the species will be reflected in the lifetime of the donor and acceptor facilitating FRET. In the current QD-GFP system, is suitable to detect trypsin protease available in the reaction medium. The lifetime of FRET facilitating QD and GFP was modified upon digestion of the linker between the histag and GFP through protease activation. Changing the enzyme concentration in solution, we observe that the lifetime of the QD-GFP complex follows a trend of decreasing back to the initial GFP lifetime, as follows from Figures 3b and d. This enables us to use the enzymatic activity to increase the distance among the donor-acceptor pair and thus control the FRET efficiency (Figure 3a). As the optimum working condition of the trypsin protease is at 37 C, below this point through the deactivation of the protease no modification of the life time of the acceptor as shown in Figure 3b. The control experiments were followed in the same manner except for the heat treatment.

Conclusions

We have shown the excitonic composite structures of QD-GFP complexes. The FRET-mediated light harvesting in this composite resulted in up to 15-fold enhancement in the emission of the acceptor protein. The lifetime modifications of the donor-acceptor pair have been supported by the theoretical analysis based on dipole-dipole interaction. Furthermore, the trypsin enzyme was implemented for controlling the energy transfer, breaking the bond in between the dot and the protein, as a

promising tool for development of the next generation nanosensor coupled with functional proteins. This research area is especially important for showing new functionalities and opportunities for protein-QD based assemblies to be utilized in bioimaging and targeted delivery applications in biomedicine. The ability of tuning the QD fluorescence using the functionalities of the coupled proteins will be useful not only for targeted drug delivery but also for guided diagnostics-treatment.

Cytotoxicity and biological incompatibility are main drawbacks for the utilization of QDs for biological and medical applications.[23] In this respect, creating a protein based nanohybrid of a photoprotein with QD would have increased lifetime and enhanced biocompatibility. QD-GFP nanohybrids benefitfrom the biocompatibility of GFP and long fluorescent lifetime of QD. QD-GFP nanohybrid could be a promising tool for bioimaging with enhanced functionality. Additionally, the ease of tunability of their biochemical and optical properties through protein engineering makes photoproteins better candidates for coupling with QDs compared to currently available synthetic dyes.

With the current approach ZnCdSe QDs are also shown to be good candidates for the excitation of the photoproteins. Compared to the other QDs, ZnCdSe provides a better overlap with the photoproteins excitation spectra. One of the most important contributions was made for replacing chemiluminescence to pump a photoprotein with a QD photoluminescence based FRET. Considering the strong optical emission properties and fluorescence lifetime of QDs, this approach provides an opportunity for a more efficient and flexible emission enhancement for photoproteins. However, there are still challenges including potential toxicity risk induced by the QD to biological systems and issue of designing better linkers to control the attachment of photoproteins to QDs.

Hybridization of the photoprotein or other proteins with the nanostructures may enable opportunities to build functional assemblies. Not only the photoproteins but also many enzymes and proteins involved in photo-activated biological events can be tuned and enhanced by using light harvesting nanoparticles.

Acknowledgement

This work is supported by the National Research Foundation of Singapore under Grant No. NRF-CRP-6-2010-2 and NRF-RF-2009-09 and the Singapore Agency for Science, Technology and Research (A*STAR) SERC under Grant No. 112 120 2009. HVD also gratefully acknowledges ESF EURYI and TUBA.

Notes and references

[a] *Luminous! Center of Excellence for Semiconductor Lighting and Displays, School of Electrical and Electronic Engineering, School of Physical and Mathematical Sciences, Nanyang Technological University, Nanyang Avenue, Singapore 639798, Singapore,*

[b] *Department of Physics, Department of Electrical and Electronics Engineering, and UNAM – Institute of Materials Science and Nanotechnology, Bilkent University, TR-06800, Ankara, Turkey,* volkan@bilkent.edu.tr *and* urartu@mit.edu

[c] *Physical Chemistry/Electrochemistry, TU Dresden, Bergstr. 66b, 01062 Dresden, Germany*

† Electronic Supplementary Information (ESI) available: [details of the quantum dot characterization, GFP-6XHis cloning (primers and cloning strategies), expression and purification, raw data of XPS analysis of the nanohybrid and TGA raw data]. See DOI: 10.1039/b000000x/

1. T. Miyashiro and E. G. Ruby, *Mol Microbiol*, 2012, **84**, 795-806.
2. G. A. Vydryakova, A. A. Gusev and S. E. Medvedeva, *Appl. Biochem. Microbiol.*, 2011, **47**, 293-297.
3. M. T. Nicolas, J. M. Bassot and O. Shimomura, *Photochem. Photobiol.*, 1982, **35**, 201-207.
4. E. A. Widder, *Science*, 2010, **328**, 704-708.
5. J. W. Hastings, *J Mol Evol*, 1983, **19**, 309-321.
6. D. Scott, E. Dikici, M. Ensor and S. Daunert, in *Annual Review of Analytical Chemistry, Vol 4*, eds. R. G. Cooks and E. S. Yeung, Annual Reviews, Palo Alto, 2011, pp. 297-319.
7. R. Borra, D. Z. Dong, A. Y. Elnagar, G. A. Woldemariam and J. A. Camarero, *J. Am. Chem. Soc.*, 2012, **134**, 6344-6353.
8. M. Drobizhev, N. S. Makarov, S. E. Tillo, T. E. Hughes and A. Rebane, *Nat. Methods*, 2011, **8**, 393-399.
9. H. Mizuno, A. Sawano, P. Eli, H. Hama and A. Miyawaki, *Biochemistry*, 2001, **40**, 2502-2510.
10. I. L. Medintz, J. H. Konnert, A. R. Clapp, I. Stanish, M. E. Twigg, H. Mattoussi, J. M. Mauro and J. R. Deschamps, *P Natl Acad Sci USA*, 2004, **101**, 9612-9617.
11. A. L. Rogach, A. Sukhanova, A. S. Susha, A. Bek, S. Mayilo, J. Feldmann, V. Oleinikov, B. Reveil, B. Donvito, J. H. M. Cohen and I. Nabiev, *Nano Letters*, 2007, **7**, 2322-2327.
12. E. R. Goldman, I. L. Medintz, J. L. Whitley, A. Hayhurst, A. R. Clapp, H. T. Uyeda, J. R. Deschamps, M. E. Lassman and H. Mattoussi, *J. Am. Chem. Soc.*, 2005, **127**, 6744-6751.
13. A. M. Dennis and G. Bao, *Nano Letters*, 2008, **8**, 1439-1445.
14. V. R. Hering, G. Gibson, R. I. Schumacher, A. Faljoni-Alario and M. J. Politi, *Bioconjugate Chem*, 2007, **18**, 1705-1708.
15. A. Rakovich, A. Sukhanova, N. Bouchonville, E. Lukashev, V. Oleinikov, M. Artemyev, V. Lesnyak, N. Gaponik, M. Molinari, M. Troyon, Y. P. Rakovich, J. F. Donegan and I. Nabiev, *Nano Letters*, 2010, **10**, 2640-2648.
16. I. Nabiev, A. Rakovich, A. Sukhanova, E. Lukashev, V. Zagidullin, V. Pachenko, Y. P. Rakovich, J. F. Donegan, A. B. Rubin and A. O. Govorov, *Angewandte Chemie-International Edition*, 2010, **49**, 7217-7221.
17. U. O. S. Seker, T. Ozel and H. V. Demir, *Nano Letters*, 2011, **11**, 1530-1539.
18. V. Lesnyak, A. Plotnikov, N. Gaponik and A. Eychmuller, *Journal of Materials Chemistry*, 2008, **18**, 5142-5146.
19. U. O. S. Seker, G. Zengin, C. Tamerler, M. Sarikaya and H. V. Demir, *Langmuir*, 2011, **27**, 4867-4872.
20. E. Yuca, A. Y. Karatas, U. O. S. Seker, M. Gungormus, G. Dinler-Doganay, M. Sarikaya and C. Tamerler, *Biotechnology and Bioengineering*, 2011, **108**, 1021-1030.
21. Y. M. Wang, J. O. Tegenfeldt, W. Reisner, R. Riehn, X. J. Guan, L. Guo, I. Golding, E. C. Cox, J. Sturm and R. H. Austin, *P Natl Acad Sci USA*, 2005, **102**, 9796-9801.
22. E. Mutlugun, P. L. Hernandez-Martinez, C. Eroglu, Y. Coskun, T. Erdem, V. K. Sharma, E. Unal, S. K. Panda, S. G. Hickey, N. Gaponik, A. Eychmuller and H. V. Demir, *Nano Letters*, 2012, **12**, 3986-3993.
23. F. M. Winnik and D. Maysinger, *Accounts Chem Res*, 2012.